14th Annual Meeting, Abu Dhabi
United Arab Emirates & Online
30 May – 02 June 2022

Permeability estimation in the low-porous rock sample using the Navier-Stokes equation at slip and no-slip conditions

Paweł Madejski
AGH University of Science and Technology, Faculty of Mechanical Engineering and Robotics
Paulina Krakowska-Madejska
AGH University of Science and Technology, Faculty of Geology, Geophysics and Environmental Protection
Corresponding author: Paweł Madejski, email: madejski@agh.edu.pl

Introduction and Motivation

Porosity and permeability are particularly important in the porous materials analysis, especially in petroleum industry, where the possibilities of hydrocarbons exploitation depend on these properties. Reservoir rocks in conventional version are mainly characterized by absolute permeability above 0.01 mD, while unconventional – below 0.01 mD. The computational methods become more popular and efficient in analyzes of fluid flow and heat transfer in the porous media. Computational fluid dynamic (CFD) gives the opportunity to assess the absolute permeabilities of rock, supporting the standard procedure: laboratory measurements of absolute permeability, as gas permeameters [1]. One of the important challenge in porous media analyzes are the research on the gas flow at microscale as estimation of the absolute permeability in tight rocks (unconventional) [2,3]. Computed X-ray tomography (CT) is one of the best laboratory technique to retrieve information about the 3D pore space of the rock. CT and CFD can become a key method in absolute permeability calculations for many types of rocks, different pore space objects (pores, fractures, etc.) and fluids [4,5].

Low-porous rock sample

CT allows extracting the geometrical model of the pore space in detail, thanks to X-ray intensity attenuation. CT data was processed to give the final output in the form of the 3D grey level image of the tight sandstone sample. Using binarization, pore space was extracted from the image and filtrated against the noise. The next stage was connected with the qualitative and quantitative interpretation of the pore space, using poROSE software [6]. Figure 1 presents the results of the object size classification regarding the object volume. Colors refer to the volume range of the objects. Only 6 objects are characterized by the volume above 5.12E5 μm³ and are marked in magenta. Pore space is poorly developed, what is reflected in very low diameter values of pores. Pores and microfractures are not very tortuous. After 3D qualitative and quantitative analysis, the most representative fragment of the pore space was extracted to build the geometrical model for the fluid flow simulations. Moreover, poROSE software was implemented to obtain a 3D geometric model in the form of STL file. Absolute permeability was measured on the cylinder plug in the laboratory using gas permeameter (Schlumberger Reservoir Laboratory) and nitrogen as a working fluid at 500 psi confining stress on the unsteady state. Absolute permeability of the analyzed sample is 0.023 mD. Total porosity from CT is equal to 2.30%, while effective porosity from the mercury porosimetry is 0.28%.

Pore sample model for CFD simulation

In the presented study, the calculations using CFD approach and solving the Navier-Stokes equations were carried out for steady-state and laminar flow with the use of Star-CCM+ software. Figure 2 presents the geometrical model of the largest object. To create a numerical mesh, the object was divided into 1,574,954 Control Volumes with polyhedral shape. The base size of the finite volume was set to 10^{-6} m, where the total height of the analyzed sample is equal to $96 \cdot 10^{-5}$ m. The mean free path of the nitrogen was calculated using gas kinetic theory. The boundary conditions were defined in the form of the pressure difference between the inlet and outlet, which represented the conditions occurring during fluid flow through the porous material.

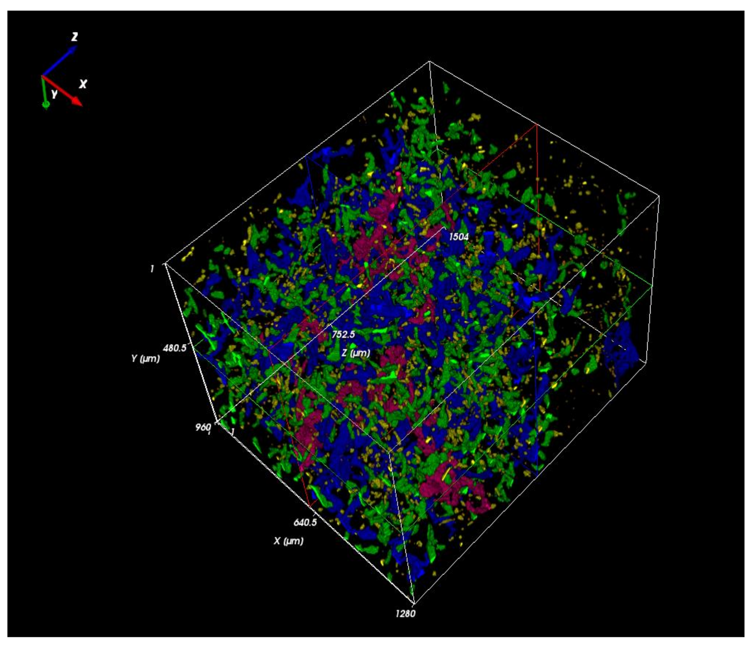

Fig. 1. Object size classification regarding object volume

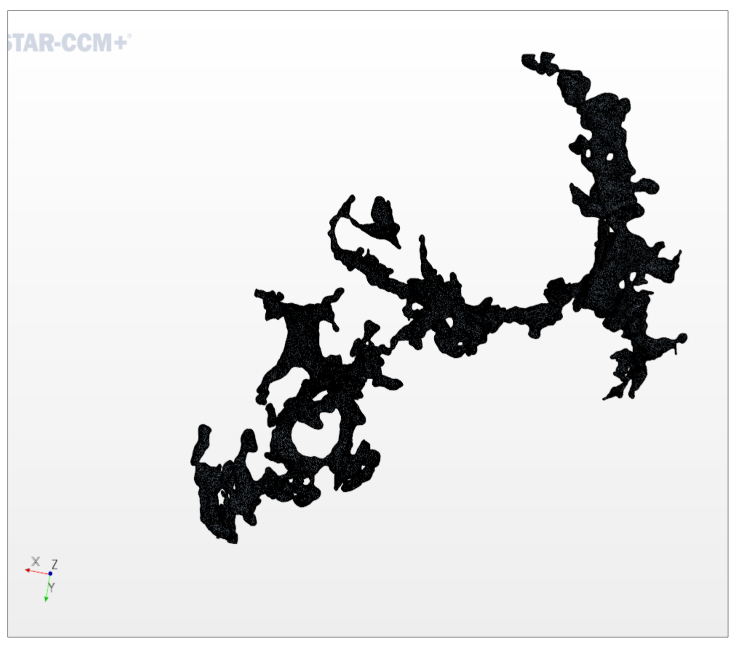

Fig. 2. Geometrical model of the pore space

Fluid flow at microscale

Flow of gas at the microscale has fundamental differences with respect to flow at the conventional scales [7,8]. The primary difference is the slip of gas at gas-solid interface. These effects are generally referred to the rarefaction and compressibility effects respectively, and are measured using non-dimensional parameters: Knudsen number (Kn), and Mach number (Ma). Rarefaction effect at microscale is a function of mean free path λ and Knudsen number. The Knudsen number is above Kn > 0.001 at the microscale owing to the small length scale L (Fig. 3).

$$Kn = \frac{\lambda}{L} \quad (1) \qquad \lambda = \frac{\kappa T}{\sqrt{2}\pi P \sigma^2} \quad (2)$$

where: κ – Boltzmann constant ($\kappa = 1.38066e-23$), J/K; T – temperature, K; P – pressure, Pa; σ – Lennard Jones characteristic length or collision diameter.

When the density of the gas is low due to reduction of pressure, then gas can start accelerate. When the Mach number is below Ma < 0.2 - 0.3, the effect of compressibility can be negligible [9,10]. The compressibility and rarefaction phenomena in gas microflows are generally coupled together, and they can have an opposite effect on each other in the slip flow and early transition regimes.

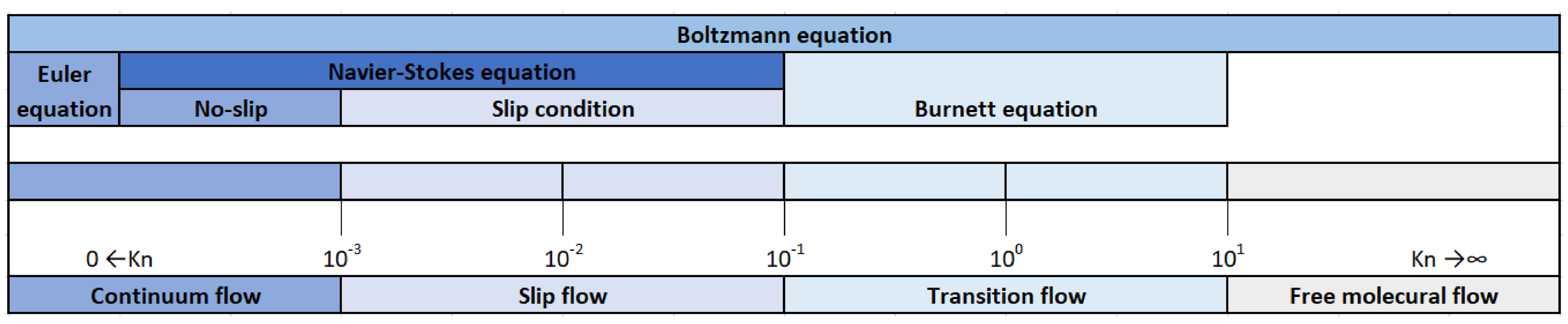

Fig. 3. Flow regimes in terms of Knudsen number

Slip flow modeling

In cases, where slip of the molecules at the pore walls is analyzed, the modeling of partial slip phenomenon is considered in the model. Boundary conditions described by partial slip (Maxwell) model and tangential momentum accommodation coefficient (σ_v) gave the opportunity to calculate slip velocity at the walls [7,11]:

$$u_{slip} = u_{gas} - u_{wall} = \frac{2-\sigma_v}{\sigma_v} L \frac{\partial u}{\partial n} \quad (3)$$

where:

u_{slip} – tangential slip velocity, m/s
u_{gas} – velocity of gas at the wall, m/s
u_{wall} – wall velocity, m/s
σ_v – tangential momentum accommodation coefficient
L – mean free path of the gas

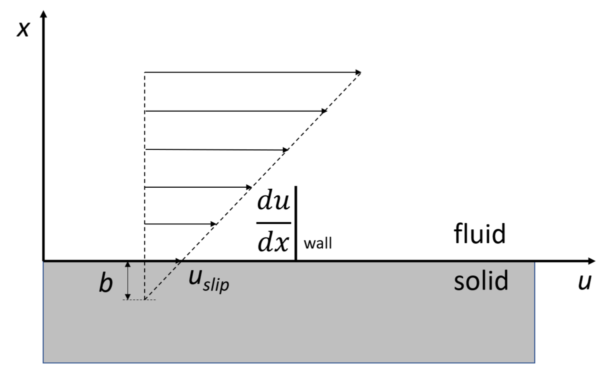

Fig. 4. Slip boundary condition

Permeabiliity estimation

Absolute permeability of incompressible fluid at steady-state:

$$K = \frac{\dot{V} \mu L_s}{A_s(p_1 - p_2)} \quad (4)$$

Volumetric flow rate calculated in CFD simulation at the sample outlet:

$$\dot{V} = \int_{A_p} u dA \quad (5)$$

Permeability, where a gas is used as a working fluid, together with partial slip effect at the sample walls:

$$K = \frac{2 p_2 \mu L_s \dot{V}}{A_s({p_1}^2 - {p_2}^2)} \quad (6)$$

Fluid is considered as a compressible medium, compressibility factor and equation of state need to be adopted in the following form:

$$\frac{p\dot{V}}{ZT} = \frac{p_{sc}\dot{V}_{sc}}{T_{sc}} \quad (7) \qquad \dot{V} = \frac{p_{sc}\dot{V}_{sc} Z T}{p T_{sc}} \quad (8)$$

Eq. (5) can be modified to the final form used to calculate absolute permeability at different pressure of gas, taking into account compressibility of analyzed fluid:

$$K = \frac{2\dot{V}_{sc} p_{sc} Z T \mu L_s}{A_s({p_1}^2 - {p_2}^2) T_{sc}} \quad (9)$$

Results

The impact of TMAC on total gas flow rate was investigated. In partial slip model, TMAC value was adopted in the whole possible range from 0.1 to 0.9. The values of velocity inside the pore channel increased with lower TMAC coefficient and higher slip velocity calculated using Eq. (3). Results are presented in Figure 5.

In Figure 6 results of absolute permeability estimation using Eq. (4) and Eq. (6) for water and nitrogen, respectively are shown. Figure 7 presents results of permeability calculations using Eq. (9) for compressible gas.

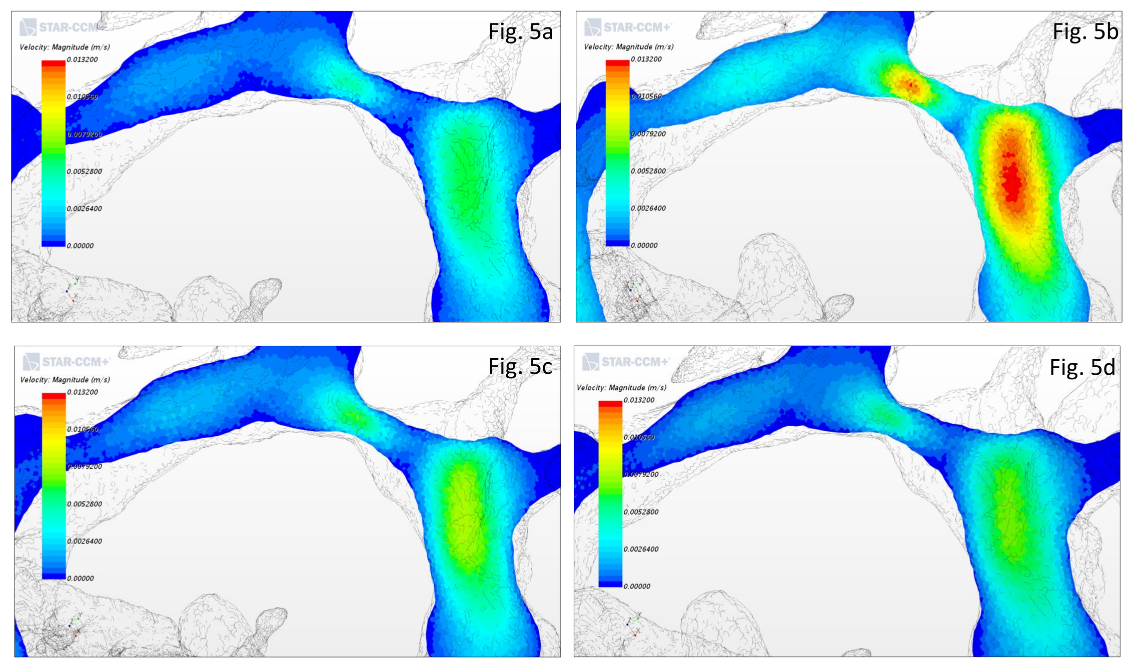

Fig. 5. Velocity distribution in the pore channel calculated using non-slip conditions (a) and partial slip model with different TMAC values equal to 0.9 (b), 0.5 (c) and 0.1 (d).

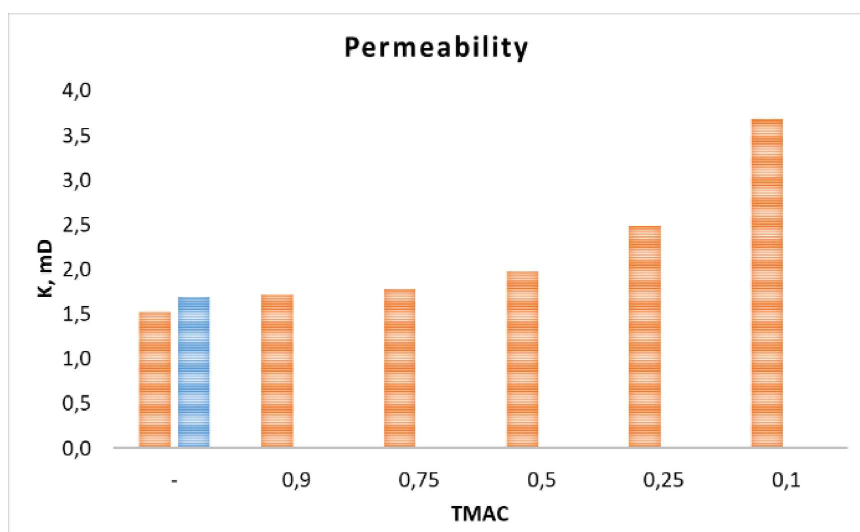

Fig. 6. Permeability K for incompressible gas (orange) using Eq. (6) and different TMAC values (non-slip, 0.1 to 0.9), and for water (blue) Eq. (4)

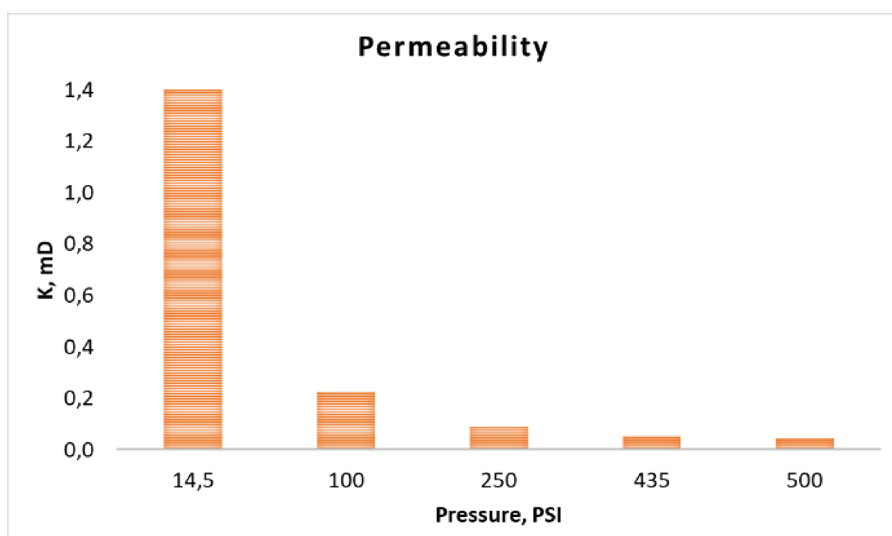

Fig. 7. Permeability K for compressible gas using Eq. (9) for different average pressure values (14.5 to 500 PSI)

Conclusions

Values of absolute permeability were determined using proposed approach and CFD simulations results. Input data to determine this values was volumetric flow rate from CFD simulations. Permeability calculated for case with liquid (water) is close to the values obtained for gas (nitrogen) and non-slip boundary conditions as well as partial slip model with TMAC=0.9. In cases for low porous rocks, not all standard measuring methods can be used for absolute permeability estimation. Permeability calculated for compressible gas, can be dozen times smaller, than value obtained at standard conditions. In analyzed case, the calculated absolute permeability of low porous rock sample is equal to 0.04 mD and comparable to measured value 0.023 mD from gas permeameter in laboratory conditions and at confining pressure 500 PSI. Absolute permeability is very important parameter and can give many answers about potential of gas exploitation from technical, environmental and economical point of view. The presented approach combining CT, CFD, equation of state and compressible gas properties allows determining absolute permeability at slip and no-slip conditions. CFD gives also the possibility to investigate and analyze slip velocity occurring at the wall of pore channels with really small diameter. The basic input data is 3D model of the pore space, extracted using highly specialized software poROSE (porous materials examination SoftwarE).

Acknowledgments: Research results presented in this paper was partially funded by by MEiN subsidy no. 16.16.130.942 (Faculty of Mechanical Engineering and Robotics, AGH UST).

References: [1] Han, G., Chen, Y., Liu, X., 2019, Investigation of Analysis Methods for Pulse Decay Tests Considering Gas Adsorption, Energies, 12(13), 2562; [2] Cao, N., Lei, G., Dong, P., Li, H., Wu, Z., li, Y., 2019, Stress-Dependent Permeability of Fractures in Tight Reservoirs, Energies, 2019, 12(1), 117; [3] Madejski, P., Krakowska, P., Habrat, M., Puskarczyk, E. and Jędrychowski, M., 2019, Permeability determination in tight rock sample using novel method based on partial slip modelling and X-ray tomography data, International Journal of Numerical Methods for Heat & Fluid Flow, Vol. ahead-of-print, No. ahead-of-print, DOI: 10.1108/HFF-11-2018-0711; [4] Islam, A., Chevalier, S., Sassi, M., 2018, Structural characterization and numerical simulations of flow properties of standard and reservoir carbonate rocks using micro-tomography, Computers & Geosciences, 113, pp. 14-22; [5] Wu, Y., Tahmasebi, P., Lin, Ch., Muhammad Munawar, M.J., Cnudde, V., 2019, Effects of micropores on geometric, topological and transport properties of pore systems for low-permeability porous media, J. Hydrology, 575, pp. 327-342; [6] Madejski, P., Krakowska, P., Habrat, M., Puskarczyk, E. and Jędrychowski, M., 2018, Comprehensive Approach for Porous Materials Analysis Using a Dedicated Preprocessing Tool for Mass and Heat Transfer Modeling, J. Thermal Science, 27, pp. 479–486; [7] Agrawal A., 2011, A Comprehensive Review on Gas Flow in Microchannel. Int J of Micro-Nano Scale Transport, 2/1, 1–40; [8] Beskok A., Karniadakis G.E. and Trimmer W., 1996, Rarefaction and Compressibility Effects in Gas Microflows. J of Fluids Engeenering, 118, 448–456; [9] Li and Guo, 2000, Characteristics of frictional resistance for gas flow in microtubes, Proceedings of Symposium on Energy Engineering in the 21st Century, Paris, France, 1–6, 658–664; [10] Colin, S., 2004, Rarefaction and compressibility effects on steady and transient gas flows in microchannels, Microfluidics and Nanofluidics, 1/3, 268–279; [11] Civan, F., 2011, *Porous media transport phenomena,* John Wiley & Sons Inc., New Jersey.